

Localized superconductivity and Little-Parks effect in superconductor/ferromagnet hybridsA. Yu. Aladyshkin,^{1,2,*} D. A. Ryzhov,² A. V. Samokhvalov,² D. A. Savinov,² A. S. Mel'nikov,² and V. V. Moshchalkov¹¹*INPAC—Institute for Nanoscale Physics and Chemistry, Nanoscale Superconductivity and Magnetism and Pulsed Fields Group, K.U. Leuven, Celestijnenlaan 200D, B-3001 Leuven, Belgium*²*Institute for Physics of Microstructures, Russian Academy of Sciences, 603950 Nizhny Novgorod, GSP-105, Russia*

(Received 11 January 2007; revised manuscript received 20 February 2007; published 22 May 2007)

On the basis of Ginzburg-Landau theory we investigate order-parameter (OP) nucleation in superconducting films of a finite thickness in the presence of inhomogeneous magnetic fields induced by ferromagnetic nanoparticles. In particular, we consider a generic system, consisting of a small perpendicularly magnetized nanoparticle, placed at a height h above the disk center. We study the oscillatory dependence of the critical temperature T_c of the disk on an external magnetic field H , similar to the classical Little-Parks effect [Phys. Rev. Lett. **9**, 9 (1962)]. Two OP nucleation regimes have been found: an appearance of superconductivity either near the disk center (under the magnetic particle) or near the disk edge. Switching between these regimes at varying the external field has been shown to result in an abrupt modification of the $T_c(H)$ dependence—both the amplitude and the period of the Little-Parks oscillations become much larger, provided that the OP pattern is localized under the particle and $R \gg h$, R is the disk radius. The OP nucleation near the magnetic particle is strongly suppressed by increasing the film thickness. Using both analytical and numerical approaches we have found the range of system parameters that are optimal for the experimental observation of the different regimes of localized superconductivity in this hybrid system.

DOI: [10.1103/PhysRevB.75.184519](https://doi.org/10.1103/PhysRevB.75.184519)

PACS number(s): 74.62.-c, 74.25.Dw, 74.78.Fk

I. INTRODUCTION

The Little-Parks effect,¹ i.e., the oscillations of the critical temperature T_c of multiply connected superconducting samples in an applied magnetic field H , is one of the striking phenomena that demonstrate the coherent nature of the superconducting state. Such oscillatory behavior of the $T_c(H)$ has been shown to be inherent also to singly connected mesoscopic samples² (with a lateral size of the order of several coherence lengths ξ) and to hybrid superconductor/ferromagnet (S/F) systems with magnetic dots^{3–10} that create the “magnetic template” for the nucleation of superconducting order parameter (OP). In all these cases the oscillations in the $T_c(H)$ line are caused by phase transitions between states with different vorticities L , characterizing the circulation of the phase of the OP. Fluxoid quantization, peculiar to all superconducting systems, could provide not only critical temperature oscillations, but also quantized levitation states in S/F hybrids.¹¹

Recent theoretical investigations of vortex matter and localized superconductivity in hybrid S/F structures were in most cases based on an idealized assumption of an infinitely small thickness D of superconducting films.^{6–10,12,13} Such a simplification allows the spatial variation of the OP over the sample thickness and the influence of the in-plane component B_{\parallel} of the magnetic field on the superconductivity nucleation both to be neglected. As a result, the OP patterns and the phase-transition line $T_c(H)$ are fully determined by the spatial distribution of the transverse B_{\perp} component, perpendicular to the film plane. Depending on the particular geometry of the stray field, these OP patterns can take the form of open-ended or closed channels,^{10,12–16} located near the regions where the component B_{\perp} is close to zero.

However, as the thickness of the superconducting film increases it can become comparable to the characteristic

length scale of the OP variation imposed by both the out-of-plane and in-plane components of the magnetic field. Thus, the OP distribution in superconducting films of a finite thickness is expected to be inhomogeneous both in the lateral and transverse directions. As a result, the critical temperature of the OP appearance and the OP patterns are strongly affected by all components of the magnetic field. In addition, both field components B_{\parallel} and B_{\perp} cannot be considered as uniform over the film thickness if the D value is of the order of the typical length scales characterizing the magnetic landscape (either the interdomain wall distance, the magnetic dot diameter, or the thickness of the ferromagnetic films and dots). The influence of the sample thickness on OP nucleation in planar, large-area S/F hybrids containing certain stripe-type domain structures inside the ferromagnetic film was studied recently in Ref. 17. A similar effect (an effective weakening of the influence of the nonuniform magnetic field on the OP nucleation due to a finite thickness of the superconducting film) can also be expected in hybrid S/F systems with magnetic dots. Thus, the increase in the D value is expected to suppress superconductivity localized near the magnetic dot, and to promote the appearance of alternative OP patterns, localized at sample imperfections, boundaries, cavities, etc. As a result, the phase boundary $T_c(H)$, corresponding to the formation of the OP pattern with the highest T_c for any H value, could have quite exotic shape due to the possible interplay between various OP structures with particular dependencies of the critical temperature on the external field and the sample thickness.

The main goals of the paper are as follows:

(i) to demonstrate that an appearance of superconductivity in hybrid S/F systems can occur in different ways (e.g., the formation of the OP either at the superconducting sample perimeter or close to a magnetic dot);

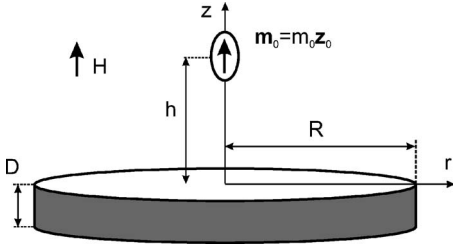


FIG. 1. A schematic representation of the S/F system under consideration.

(ii) to investigate the shape of the phase-transition line $T_c(H)$ in a system with two competing regimes of the OP nucleation; and

(iii) to study the transformation of the $T_c(H)$ line at varying the parameters of the magnetic dot and the thickness of the superconductor.

The paper is organized as follows. Firstly, we introduce the set of basic equations in Sec. II. In Sec. III we discuss qualitatively two possible regimes of OP nucleation in the system under consideration prior to starting detailed calculations. In Sec. IV we present the results of an approximate analytical analysis of OP nucleation in thin and thick large-area superconducting films in the presence of a small magnetic particle and the estimates of the phase boundary $T_c(H)$ in this limits. The competition between two nucleation regimes, based on direct numerical calculations using linearized Ginzburg-Landau theory, is studied in Sec. V. Finally, we make some concluding remarks.

II. MODEL

We consider a small magnetic dot, placed at a height h above the center of a superconducting disk of a finite radius R and thickness D (Fig. 1). The opposite case, when both the lateral size of the superconductor and the diameter of the magnetic dot are of the same order of magnitude, was considered in Refs. 7–9. For the sake of simplicity, we choose the magnetic moment $\mathbf{m}_0 = m_0 \mathbf{z}_0$ of the dot as well as the external field $\mathbf{H} = H \mathbf{z}_0$ to be perpendicular to the disk plane [here (r, θ, z) is the cylindrical reference system]. As an example, perpendicularly magnetized magnetic dots can be prepared using multilayered Co/Pt films.¹⁸ Due to the non-zero distance h between the particle and the top surface of the superconducting disk we can exclude the exchange interaction (for a review, see Refs. 19–21) and focus on the orbital effect.

The conditions for the appearance of superconductivity as well as the spatial profile of the OP wave function $\Psi(\mathbf{r})$ follow from the linearized Ginzburg-Landau equation,

$$-\left(\nabla - \frac{2\pi i}{\Phi_0} \mathbf{A}(\mathbf{r})\right)^2 \Psi = \varepsilon \Psi, \quad \varepsilon = \frac{1}{\xi^2(T)}. \quad (1)$$

Here $\mathbf{A}(\mathbf{r})$ is the vector potential corresponding to the total magnetic field $\mathbf{B}(\mathbf{r}) = \text{rot } \mathbf{A}(\mathbf{r})$, $\Phi_0 = \pi \hbar c / e$ is the flux quantum, $\xi(T) = \xi_0 (1 - T_c / T_c)^{-1/2}$ is the superconducting coherence length, and T_c is the critical temperature of the bulk

superconductor at $B=0$. Note that in Eq. (1) we neglect the corrections to the vector potential caused by the screening currents, since the supercurrents are proportional to $|\Psi|^2$ and result in higher-order terms omitted in our approximation.²² Hence the superconductor cannot affect the ferromagnet near the phase-transition line and the magnetization of the dot remains unaltered.

Provided that the dot size is smaller than the other relevant length scales (the point magnetic dipole approximation), the vector potential $\mathbf{a}^m(\mathbf{r})$, corresponding to the stray field of the dot, can be written as

$$a_{r,z}^m = 0, \quad a_\theta^m(r, z) = \frac{m_0 r}{[r^2 + (z-h)^2]^{3/2}}.$$

Choosing the gauge $A_\theta(r, z) = a_\theta^m(r, z) + Hr/2$, $A_r = A_z = 0$, it can be seen that the Schrödinger-like Eq. (1) does not depend on the θ coordinate, and the solution of Eq. (1) can generally be found in the form of giant (multiquanta) vortices $\Psi(\mathbf{r}) = f_L(r, z) \exp(iL\theta)$, where L is the angular momentum of the Cooper pairs.²³

The absolute value of the OP wave function, $f_L(r, z)$, can be determined from the following two-dimensional equation:

$$-\frac{\partial^2 f_L}{\partial r^2} - \frac{1}{r} \frac{\partial f_L}{\partial r} - \frac{\partial^2 f_L}{\partial z^2} + U(r, z) f_L = \varepsilon(L) f_L,$$

$$U(r, z) = \left(\frac{2\pi}{\Phi_0} A_\theta(r, z) - \frac{L}{r} \right)^2. \quad (2)$$

A set of eigenvalues $\varepsilon_n(L)$ of Eq. (2) for any H values gives us a set of critical temperatures $T_c^{L,n} = T_{c0} [1 - \xi_0^2 \varepsilon_n(L)]$, corresponding to the appearance of various OP patterns $\Psi_{L,n} = f_{L,n} \exp(iL\theta)$. We will define the critical temperature as the highest possible value $T_c = \max_{L,n} \{T_c^{L,n}\}$.

Assuming that the superconducting sample has an insulating coating, boundary conditions corresponding to zero normal derivatives of the OP at all surfaces (the Neumann-type boundary conditions) should be applied;

$$\left. \frac{\partial f_L}{\partial z} \right|_{z=0, -D} = 0, \quad \left. \frac{\partial f_L}{\partial r} \right|_{r=R} = 0. \quad (3)$$

Following Ref. 10 we will use the parameter $N_f = 4\pi m_0 / (3\sqrt{3}\Phi_0 h)$ characterizing the dipole moment in dimensionless units and the value $B_0 = 2m_0/h^3$ as a unit for the magnetic field.

III. TWO DIFFERENT OP NUCLEATION REGIMES: QUALITATIVE ANALYSIS

We start with a preliminary consideration of the simplest case $D \rightarrow 0$ in order to better reveal the effects expected to arise from the possible switching between different OP nucleation regimes.

Obviously, there are only two favorable regimes of the OP nucleation in the system under consideration (without any defects inside the superconductor), which can be clearly separated in the particular case $D \ll h \ll R$ and described as follows:

(i) The formation of the OP in the central part of the disk under the dipole (magnetic-dot-assisted superconductivity).

(ii) The formation of the OP at the outer perimeter of the superconducting disk (edge superconductivity). Edge nucleation takes place even in the absence of the magnetic dot and this regime is weakly influenced by the presence of a magnetic dot provided $R \gg h$.

The mechanism of the magnetic-dot-assisted superconductivity is associated with the field compensation effect and it appears to be important only for negative H values.¹⁰ For positive H values, edge superconductivity becomes the dominant regime. This regime should also dominate for large negative H values. Indeed, for quite large, negative H values, the z component of the field has its minimum at the disk center. If the size of the center OP nucleus is much smaller than the other relevant length scales, the critical temperature can be estimated as

$$1 - \frac{T_c^{\text{cent}}}{T_{c0}} \approx \frac{2\pi\xi_0^2}{\Phi_0} |H + B_0|.$$

The value T_c^{cent} should be compared with the standard expression for the critical temperature for the edge nucleation regime in the limit $R \gg h$

$$1 - \frac{T_{c3}}{T_{c0}} \approx 0.59 \frac{2\pi\xi_0^2}{\Phi_0} |H|,$$

which corresponds to the $H_{c3}(T)$ field (see, e.g., Ref. 22). Due to the different slopes dT_c^{cent}/dH and dT_{c3}/dH and the different offsets, we get a point $H=H_1^*$ where both critical temperatures are equal: $H_1^* \approx -2.44B_0$. The edge OP nucleation regime therefore apparently dominates both at positive and large negative field values. Hence we conclude that there is a second switching field H_2^* somewhere between $H=-B_0$ and $H=0$. The above arguments allow us to separate three field regions characterized by different types of OP nucleation.

Only in the intermediate field range $H_1^* < H < H_2^*$ does the highest critical temperature corresponds to a giant vortex located near the magnetic particle. It is the only regime in which the field inhomogeneity and the finite sample thickness should affect the spatial structure of such vortices and the critical temperature of their appearance. Outside this range, i.e., at $H < H_1^*$ and $H > H_2^*$, the OP nucleation in a large-area disk should take place near the edge of the disk and it should be practically independent of the parameters of the magnetic particle (if $R \gg h$). The dependence of the threshold fields H_1^* and H_2^* on the magnetic dot parameters and on the sample thickness will be considered in Sec. V.

It should be noted that we cannot exclude the scenario in which patterns with different OP profiles and different L values will coexist. Normally, as soon as the OP structure corresponding to the highest critical temperature appears in the sample, the amplitude of this solution starts to grow as the temperature decreases. Generally speaking, it should prevent the appearance of OP structures with the lower critical temperatures. However, in the important particular case $R \gg h$ two eigenfunctions of the linearized Ginzburg-Landau equation, corresponding to the different nucleation regimes, are

strongly spatially separated and their nucleation can occur almost independently. Therefore, the resulting phase boundary, measured experimentally, will significantly depend on the experimental conditions, the locations of the contact pads, etc., since the geometry of the sample and the measuring methods determine the sensitivity of the setup to the appearance of certain types of localized superconductivity. The formation of giant vortex states mentioned above could certainly be possible if the critical temperature corresponding to some particular solution exceeds the critical temperature T_{c2} of the appearance of the delocalized superconductivity

$$1 - \frac{T_{c2}}{T_{c0}} = \frac{2\pi\xi_0^2}{\Phi_0} |H|,$$

which corresponds to the conventional $H_{c2}(T)$ line in the H - T diagram. So in order to understand the possibility of observing the magnetic-dot-assisted superconductivity experimentally, the predicted phase boundary $T_c(H)$ should be compared with the reference lines $T_{c2}(H)$ and $T_{c3}(H)$.

IV. SUPERCONDUCTIVITY ASSISTED BY MAGNETIC DOT: ANALYTICAL APPROACH

In this section we focus on the consideration of the magnetic-dot-assisted superconductivity in large-area disks, assuming that the superconducting OP is located in the central part of the disk. In this case the critical temperature of the sample depends on the characteristics of the inhomogeneous magnetic field produced by the dot and the sample thickness D rather than on the lateral size of the disk R . So, one can neglect the effect of the disk edge and consider the problem of Eq. (2) with the boundary condition

$$f_L(r, z)|_{r \rightarrow \infty} = 0.$$

A. Thin superconducting films

Provided that the film thickness D is smaller than the characteristic length scale of the OP variation in the z direction, the OP distribution can be considered almost uniform over the film thickness. Thus, we can develop a perturbation theory in order to take into account the effect of the in-plane magnetic-field components on the critical temperature.

For this purpose we expand the vector potential distribution $A_\theta(r, z) = a_\theta^m(r, z) + Hr/2$ into Taylor series near the middle plane of the superconducting film (at $z^* = -D/2$)

$$A_\theta(r, z) \approx A_\theta(r, z^*) - B_r|_{r, z^*} (z - z^*) + \frac{1}{2} \left(\frac{\partial B_r}{\partial z} \right)_{r, z^*} (z - z^*)^2 + \dots \quad (4)$$

After substitution of expansion (4) into Eq. (2) and averaging over the film thickness, we get the following Sturm-Liouville problem:

$$-\frac{d^2 g_L}{dr^2} + V(r)g_L = \frac{1}{\xi^2(T)} g_L, \quad g_L(r) = \frac{\sqrt{r}}{D} \int_{-D}^0 f_L(r, z) dz. \quad (5)$$

The potential-well profile $V(r)=V_0(r)+V_{\parallel}(r)$ in Eq. (5) averaged over the thickness consists of two contributions. The dominant term

$$V_0(r) = \frac{\phi_L^2(r)}{r^2} - \frac{1}{4r^2}, \quad \phi_L(r) = \frac{2\pi r A_{\theta}(r, z^*)}{\Phi_0} - L$$

is determined by the vector potential distribution $A_{\theta}(r, z^*)$, i.e., the $V_0(r)$ profile is sensitive to the z component of the magnetic field only. This term is definitely D dependent, since the variation in the D value results in a change of the distance between the magnetic particle and the middle plane $z=z^*$. The perturbation term

$$V_{\parallel}(r) = \frac{\pi^2 D^2}{3r^2} \left(\frac{r^2 B_r^2}{\Phi_0^2} - \frac{r(B_r)_z' \phi_L(r)}{\Phi_0 2\pi} \right)$$

allows us to study the effects of the in-plane field component B_r on the nucleation of superconductivity. The limit $D \rightarrow 0$ and $N_f \gg 1$ has been previously considered in Ref. 10. Provided that $-B_0 < H < 0$, the OP is localized in the region close to the circle of the radius r_0 , where the z component of the total magnetic field vanishes, $B_z(r_0)=0$. This local approximation is valid when the typical width ℓ_r of the OP structure is much less than the characteristic scale of the magnetic-field distribution,

$$\left| \frac{(B_z)_r''}{(B_z)_r'} \ell_r \right|_{r=r_0} \ll 1 \quad \text{and} \quad \frac{\ell_r}{r_0} \ll 1.$$

Following Ref. 10 we expand the value $\phi_L(r)$ in powers of $r-r_0$,

$$\phi_L(r) \approx \phi_L(r_0) + \frac{\pi r_0 (B_z)_r'}{\Phi_0} (r-r_0)^2,$$

and rewrite the potential wells $V_0(r)$ and $V_{\parallel}(r)$ in the vicinity of the point r_0 ,

$$V_0(r) \approx \frac{1}{\ell_r^2} \left[\frac{(r-r_0)^2}{\ell_r^2} - Q_L \right]^2 - \frac{1}{4r_0^2},$$

$$V_{\parallel}(r) \approx V_{\parallel}(r_0) = \frac{D^2}{6\ell_r^4} Q_L + \frac{\pi^2 D^2 B_r^2}{3\Phi_0^2},$$

where the field B_r and the derivative $(B_z)_r' = (B_r)_z'$ are taken at the point $r=r_0$, $z=z^*$ and the parameters ℓ_r and Q_L are given by the expressions

$$\ell_r = \sqrt[3]{\frac{\Phi_0}{\pi |(B_z)_r'|}}, \quad Q_L = -\phi_L(r_0) \sqrt[3]{\frac{\Phi_0}{\pi r_0^3 (B_z)_r'}}.$$

Note that the characteristic width ℓ_r of the OP pattern is determined by the applied magnetic field, while the parameter Q_L depends on both H and L values.

Introducing a coordinate $\tau=(r-r_0)/\ell_r$ we can reduce Eq. (5) to the following universal form:

$$-\frac{d^2 g_L}{d\tau^2} + (\tau^2 - Q_L)^2 g_L = \varepsilon(Q_L) g_L, \quad (6)$$

where

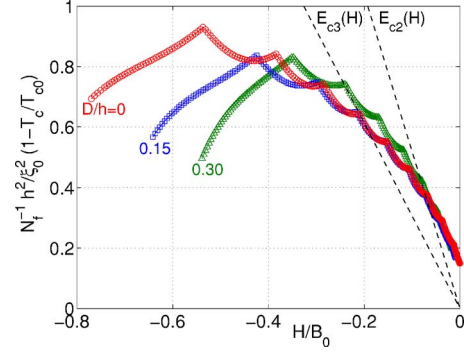


FIG. 2. (Color online) The phase boundaries $T_c(H)$ for the S/F hybrid with $N_f=10$ and $D/h \rightarrow 0$ (\circ), $D/h=0.15$ (\square), and $D/h=0.30$ (\triangle), obtained from Eq. (8). The dashed lines show the reference dependencies $E_{c2}(H) = (h^2/\xi_0^2)[1 - T_{c2}(H)/T_{c0}]$ and $E_{c3}(H) = (h^2/\xi_0^2)[1 - T_{c3}(H)/T_{c0}]$, corresponding to OP nucleation either far from the edges in a bulk sample or near the sample edges, respectively.

$$\varepsilon(Q_L) = \frac{\ell_r^2}{\xi^2(T)} + \frac{\ell_r^2}{4r_0^2} - \frac{D^2}{6\ell_r^2} \left[Q_L + 2 \left(\frac{\pi \ell_r^2 B_r}{\Phi_0} \right)^2 \right]. \quad (7)$$

Thus, the critical temperature, which enters into the first term in the right-hand side of Eq. (7), is expressed via the parameters of the field distribution and the lowest eigenvalue $\varepsilon_0(Q_L)$ of the model equation (6) as follows:

$$1 - \frac{T_c(H)}{T_{c0}} = \frac{\xi_0^2}{\ell_r^2} \min_L \left\{ \varepsilon_0(Q_L) - \frac{\ell_r^2}{4r_0^2} + \frac{D^2}{6\ell_r^2} \left[Q_L + 2 \left(\frac{\pi \ell_r^2 B_r}{\Phi_0} \right)^2 \right] \right\}. \quad (8)$$

As was shown in Ref. 10, the function $\varepsilon_0(Q_L)$ is characterized by the following asymptotical behavior: $\varepsilon_0(Q_L) \approx Q_L^2 + \sqrt{-2Q_L}$ when $Q_L \ll -1$, and $\varepsilon_0(Q_L) \approx 2\sqrt{Q_L}$ when $Q_L \gg 1$. The typical $T_c(H)$ dependencies, obtained from Eqs. (6) and (8) for the different D values, are shown in Fig. 2. The increase in the film thickness reduces the number of the $T_c(H)$ oscillations lying below $T_{c2}(H)$ and $T_{c3}(H)$ lines.

Note that the local approximation used above fails for $L=0$, when the maximum of the OP wave function is located at $r=0$ and hence Eq. (8) cannot correctly describe the OP nucleation and the phase boundary $T_c(H)$ at negative H values close to $-B_0$. Nevertheless, our model is certainly valid for nonzero L values for the description of the switching between giant vortex states with different vorticities that results in the oscillatory $T_c(H)$ dependence. Actually, the variation in the external field H changes the r_0 value (i.e., the position of the OP maxima), as well as the flux through the circle of radius r_0 and hence it changes the energetically favorable winding number L . The number of T_c oscillations in the interval $-B_0 < H < 0$ is controlled by the parameter N_f , which is the dimensionless flux of the dot's field through the area with the positive field component $b_z^m(r, z=z^*)$, the radius of which is of the order of h . Strictly speaking, the period ΔH of the Little-Parks oscillations, caused by the transition between the vortex states localized near the magnetic dot, is

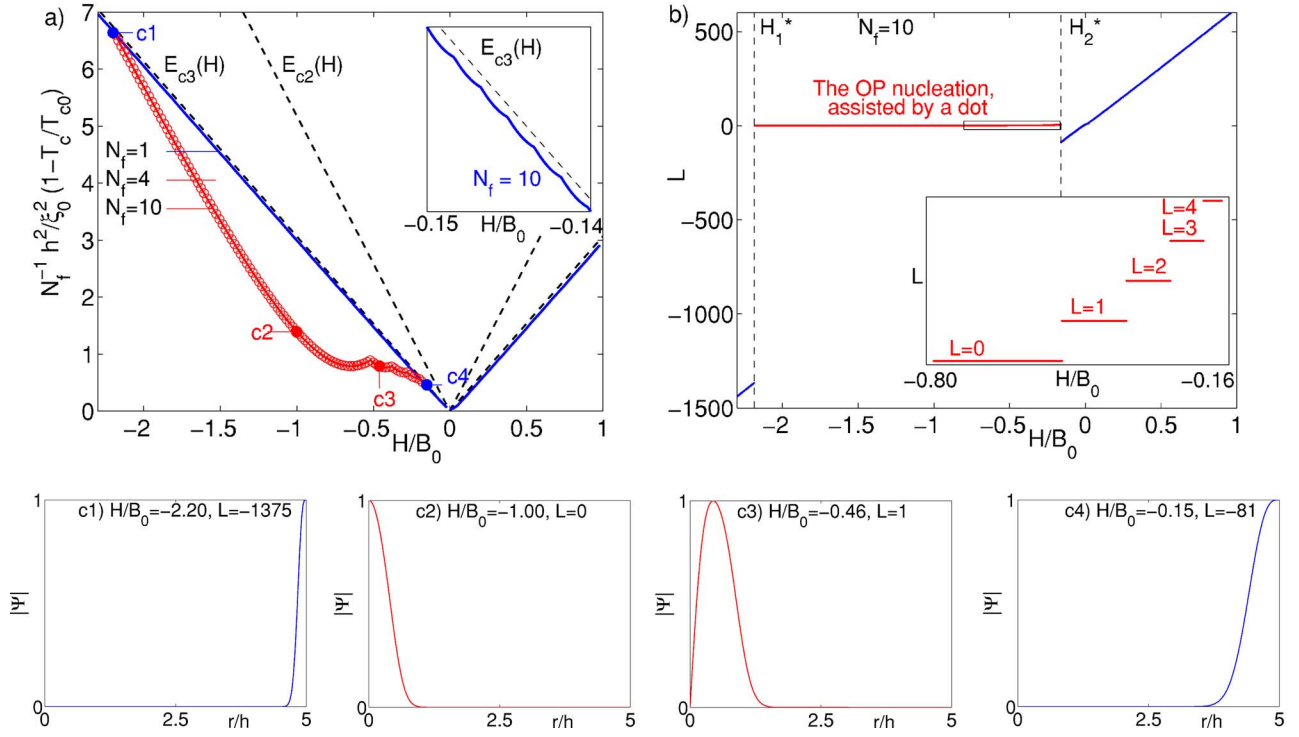


FIG. 3. (Color online) (a) The phase-transition lines $T_c(H)$, calculated numerically for $R/h=5$, $D/h \rightarrow 0$, and for $N_f=1, 10$. The curves marked by circles correspond to the center OP nucleation, while the solid curves describe the edge OP nucleation. The inset gives the zoomed part of the $T_c(H)$ line, calculated for $N_f=10$. (b) The dependence L vs H , corresponding to the case $N_f=10$, $R/h=5$, and $D/h \rightarrow 0$. The inset represents the zoomed part of the $L(H)$ line marked by the rectangle which corresponds to the transitions between the giant vortex states localized under the magnetic particle. [(c1)–(c4)] The typical OP distributions $|\Psi(r)|$ (arbitrary units), calculated for certain H values [the filled circles in panel (a)].

field dependent. However, the typical period ΔH of these oscillations can be roughly estimated as $B_0/N_f \approx \Phi_0/h^2$.

B. Thick superconducting films

Let us now discuss the opposite limit of a large film thickness. From the results of the perturbation theory presented above, we can expect that for D values of the order of h and larger the vortex states with nonzero vorticities become energetically unfavorable. The particular case of zero vorticity, $L=0$, should be examined separately. It is clear that there is a point

$$r_0/h = 0, \quad z_0/h = 1 - \sqrt[3]{B_0/|H|}, \quad (9)$$

where the total field vanishes. Provided that

$$-1 < H/B_0 < -(1 + D/h)^{-3}, \quad (10)$$

this point (r_0, z_0) is located inside the superconducting disk and it seems to be favorable for OP nucleation to occur due to the complete compensation effect. Assuming that the typical widths ℓ_r and ℓ_z of the OP along the r and z axes are much smaller than the field length scales, we can expand the vector potential $A_\theta(r, z)$ in a Taylor series near the point (r_0, z_0) , keeping only the leading term

$$A_\theta(r, z) \approx \frac{3m_0}{h^4} \left(\frac{|H|}{B_0} \right)^{4/3} r(z - z_0). \quad (11)$$

Substituting expression (11) into Eq. (2) we introduce dimensionless variables $\rho = r/(\alpha h)$ and $\zeta = (z - z_0)/(\alpha h)$ and put $\alpha^6 = (4/243)N_f^{-2}(|H|/B_0)^{-8/3}$. As a result, we get the following dimensionless equation:

$$-\frac{\partial^2 f_0}{\partial \rho^2} - \frac{1}{\rho} \frac{\partial f_0}{\partial \rho} - \frac{\partial^2 f_0}{\partial \zeta^2} + (\rho \zeta)^2 f_0 = \varepsilon f_0, \quad (12)$$

where $\varepsilon = (\alpha h / \xi)^2$. This approximation is correct if the OP is located far from both the top and the bottom film surfaces: $\ell_z \ll |z_0|$ and $\ell_z \ll |D - z_0|$. Thus, we can neglect the effect of the boundaries and consider the problem of Eq. (12) with the boundary conditions

$$f_0(\rho, \zeta)|_{\rho \rightarrow \infty} = 0, \quad f_0(\rho, \zeta)|_{\zeta \rightarrow \pm \infty} = 0.$$

The parameter α determines the localization lengths ℓ_r and ℓ_z in the lateral and transverse directions,

$$\ell_r = \ell_z = \alpha h \approx 0.5h \left(\frac{B_0}{|H|} \right)^{4/9} N_f^{1/3}. \quad (13)$$

Taking the lowest eigenvalue $\varepsilon_0 \approx 1.82$ of Eq. (12), we can estimate the phase-transition line as follows:

$$1 - \frac{T_c^*(H)}{T_{c0}} \approx 7.15 \frac{\xi_0^2}{h^2} N_f^{2/3} \left(\frac{|H|}{B_0} \right)^{8/9}.$$

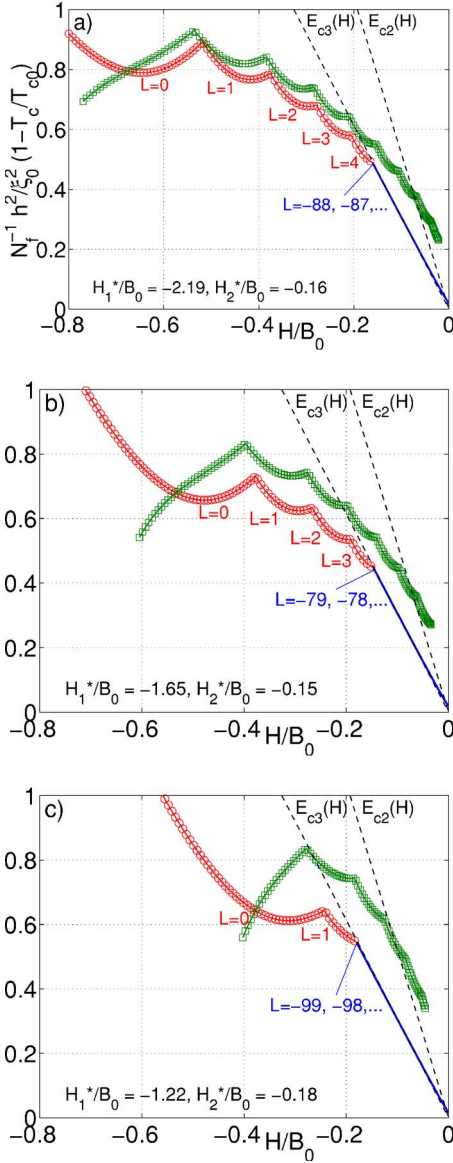


FIG. 4. (Color online) Phase boundaries $T_c(H)$, calculated numerically from Eqs. (2) and (3) for $N_f=10$, $R/h=5$, and $D/h \rightarrow 0$ (a), $D/h=0.2$ (b), and $D/h=0.5$ (c), where the curves marked by circles correspond to the formation of giant vortices localized under the magnetic particle, while the solid curves describe the OP nucleation near the disk edge. The oscillations of the critical temperature at $H > H_2^*$ caused by the edge effects are practically invisible in this scale. The lines marked by squares correspond to the $T_c(H)$ dependencies obtained analytically from Eq. (8).

Comparing this transition temperature with the critical temperature T_{c2} we obtain a criterion of the existence of the magnetic-dot-assisted nucleation regime as follows:

$$N_f \gtrsim 3 \left(\frac{B_0}{|H|} \right)^{1/3}. \quad (14)$$

According to this criterion the optimal external fields should be close to $-B_0$. Thus, taking $H \sim -B_0$, we find that for $N_f \gtrsim 3$ the critical temperature of the disk in the regime of the magnetic-dot-assisted superconductivity exceeds T_{c2} even

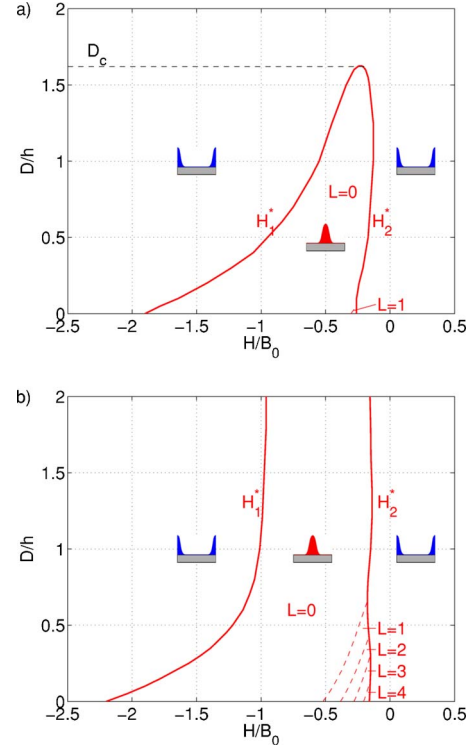


FIG. 5. (Color online) Phase diagrams in the H - D plane, calculated for the following parameters: $R/h=5$, $N_f=4$ (a), and $N_f=10$ (b). The thick solid lines are the threshold H_1^* and H_2^* lines, which separate the OP nucleation regimes: for $H_1^* < H < H_2^*$ (between these lines) the OP nucleates near the magnetic particle, while outside this range superconductivity appears at the edge of the sample. The dashed lines separate the regions with different vorticities (for the magnetic-dot-assisted regime).

for very thick films. For $N_f \lesssim 3$, superconductivity under the dot can be expected to appear only for a film thickness less than a certain critical value. To analyze the interplay between different OP nucleation regimes we also need to compare T_c^* with the temperature of the edge superconductivity nucleation T_{c3} [see Eq. (4)]. As a result, we get a critical value $N_f^c \approx 10$ that separates the nucleation regimes for thick films: for $N_f > N_f^c$ and $N_f < N_f^c$ we get the magnetic-dot-assisted and the edge nucleation regimes, respectively. In the latter case a decrease in film thickness can result in a transition to the magnetic-dot-assisted superconductivity.

V. INTERPLAY BETWEEN DIFFERENT NUCLEATION REGIMES: NUMERICAL STUDY

We now proceed with the numerical analysis of the phase-transition line $T_c(H)$ for a superconducting disk of a finite radius R and thickness D . The procedure for the numerical solution of Eqs. (2) and (3) is similar to that described in Ref. 24.

A. Phase-transition lines $T_c(H)$

Both regimes of OP nucleation mentioned above can be recognized by examining the dependence of the critical tem-

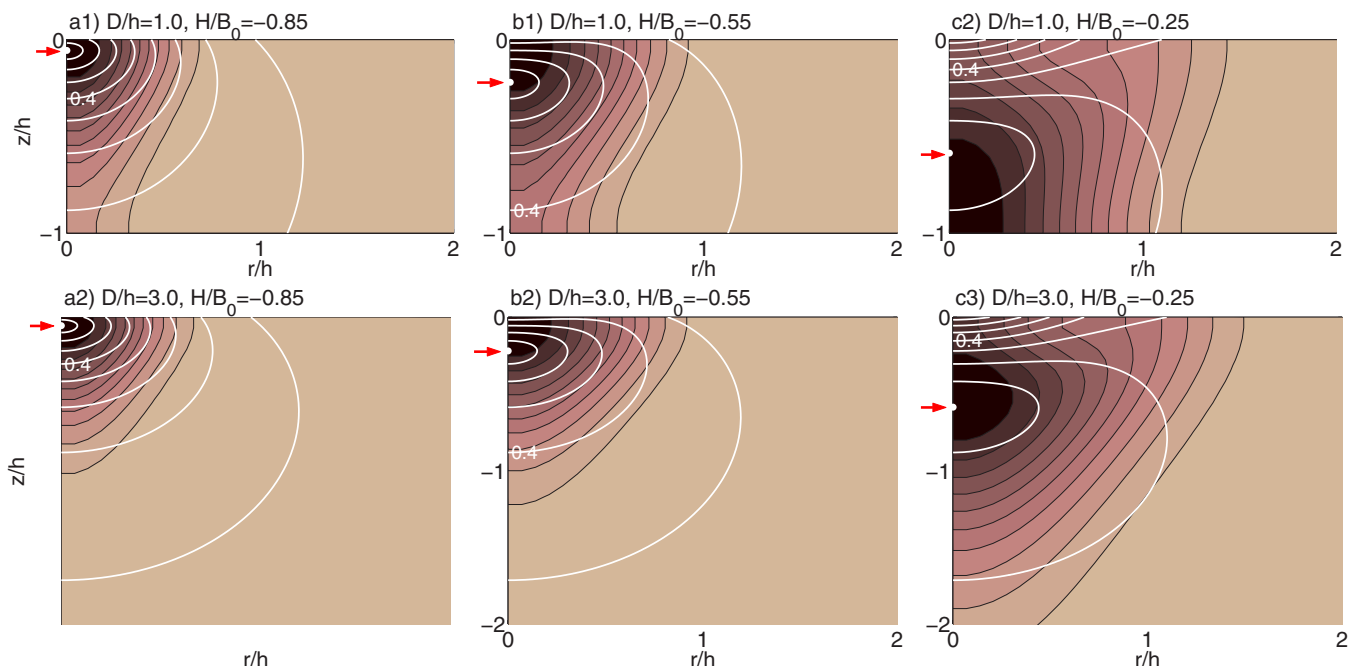


FIG. 6. (Color online) Contours of the total magnetic field $\sqrt{b_r^2 + (b_z + H)^2}/B_0 = \text{const}$ (the lines) and the OP distributions $|\Psi(r, z)|$ (arbitrary units) corresponding to the state with $L=0$. The filled circles and arrows indicate the points $r=0$, $z=z_0$, where $|B|=0$. All results correspond to $N_f=10$ and $R/h=5$, while other relevant parameters are shown in the plots. The highest $|\Psi|$ values are shown in darker shades and the lowest densities in lighter shades.

perature T_c on the external magnetic field H . Figure 3(a) shows typical $T_c(H)$ dependencies, calculated numerically for an infinitely thin superconducting disk in the presence of the magnetic dipole. In the intermediate field range (for $H_1^* < H < H_2^*$) OP nucleation takes place near the center of the sample [the curve marked by circles in Fig. 3(a)]. Otherwise, i.e., for $H < H_1^*$ or $H > H_2^*$, the superconducting OP first nucleates at the sample edge [the solid curves in Fig. 3(a)].

The kinks on the $T_c(H)$ line are due to jumps in the field dependence of the optimal vorticity L , corresponding to the state with the highest T_c [Fig. 3(b)]. The typical L vs H dependence is shown in Fig. 3(b). For the edge nucleation regime, the jumps in vorticity occur with a period $\Delta H \sim \Phi_0/R^2$. In the magnetic-dot-assisted nucleation regime we observe jumps in vorticity with a characteristic period close to the estimate given in Sec. IV A: $\Delta H \sim B_0/N_f \sim \Phi_0/h^2$. Thus, the preferable OP nucleation regime can be clearly identified by analyzing the period of the oscillations of the critical temperature vs H , provided $R \gg h$.

The phase diagrams for different disk thicknesses are shown in Fig. 4. Our numerical results appear to be in good agreement with the analytical predictions [see Eq. (8)] for relatively thin films ($D/h < 1$) and $N_f \gg 1$.

In order to describe the interplay between the two different OP nucleation regimes, we plot H - D diagrams (see Fig. 5) calculated numerically for the fixed radius of the disk $R/h=5$ and various m_0 values. Shown in these phase diagrams are the switching lines $H_1^*(D)$ and $H_2^*(D)$, which separate the regions with different types of OP nucleation. Analyzing Fig. 5 we can make the following observations.

(i) An increase in the sample thickness results in a decrease in the set of possible vortex states localized near the magnetic particle.

(ii) The zero vorticity state is the most stable dot-assisted state, and it can occur even in rather thick superconducting films. This confirms our suggestion formulated in Sec. IV B, which has been used to estimate the $T_c^*(H)$ line for bulk samples.

(iii) An increase in the D value causes a shrinking of the $|H_1^* - H_2^*|$ interval.

(iv) A change of the OP nucleation regime is accompanied by giant jumps in vorticity [see Fig. 3(b)], which take place both at $H=H_1^*$ and $H=H_2^*$. The amplitude ΔL of these jumps near the “edge-to-center” transition can be roughly estimated as $\pi R^2 H_i^*/\Phi_0$, $i=\{1, 2\}$. Similar jumps in vorticity in mesoscopic square superconductors have been obtained numerically in Refs. 8 and 9.

(v) For relatively small N_f values there exists a critical sample thickness D_c corresponding to the complete suppression of OP nucleation under the magnetic particle for any external field value [see also Fig. 3(a)]. For instance, $D_c=1.62h$ for $N_f=4$ and $R/h=5$. For $N_f \gg 1$ the critical thickness tends to infinity in qualitative agreement with our estimates in Sec. IV B.

B. OP patterns located near the magnetic particle

Let us now discuss the spatial structure of the OP patterns. Our numerical calculations demonstrate that in the intermediate H range ($H_1^* < H < H_2^*$) the OP distribution becomes strongly inhomogeneous along the z axis as the sample thick-

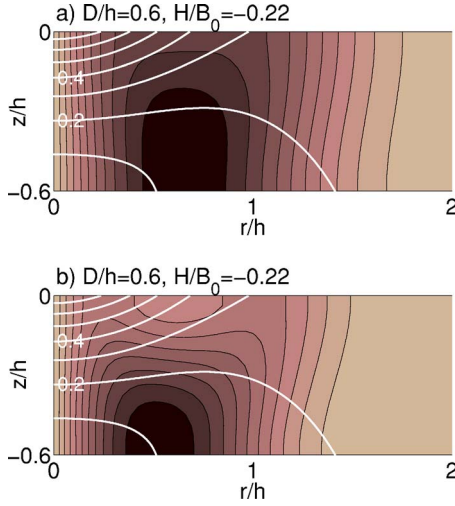


FIG. 7. (Color online) Contours of the total magnetic field $\sqrt{b_r^2 + (b_z + H)^2}/B_0 = \text{const}$ (the lines) and the OP distributions $|\Psi(r, z)|$ (arbitrary units) corresponding to the vortex solution with $L=1$. The results correspond to $R/h=5$, $D/h=-0.6$, $H/B_0=-0.22$, $N_f=10$ (a), and $N_f=20$ (b). The highest $|\Psi|$ values are shown in darker shades and the lowest densities in lighter shades.

ness becomes comparable with the characteristic OP width ℓ_z .

Figure 6 shows the OP distributions for $L=0$ for different external field values. For fields $|H| \lesssim B_0$ (the left column in Fig. 6), the point (r_0, z_0) , determined by Eq. (9), where the dipole magnetic field is compensated exactly, is situated rather close to the top film surface: $r_0=0$, $|z_0| \ll \ell_z$. Due to the boundary effect, the OP nucleus is attracted to the $z=0$ plane and the maximum of the OP distribution lies at the top film surface. A decrease in the ratio $|H|/B_0$ results in a shift of the compensation point (r_0, z_0) from the top plane. Depending on the film thickness, the OP maximum in this case shifts either to an internal point close to the compensation one, or to the bottom film surface (the middle and right columns in Fig. 6). In agreement with estimate (13), we also observe an increase in the localization lengths ℓ_r and ℓ_z in both directions with a decrease in the amplitude of the external magnetic field.

Since the leading term in the series expansion of the effective potential $U(r, z) \sim L^2/r^2$ for $L \neq 0$ and $r \ll h$ does not contain the parameters of the magnetic particle, we note that despite the inhomogeneity of the field in the z direction the asymptotic behavior of the OP should be the same as for the giant vortex in a uniform magnetic field²²: $\Psi_L(r, z) = C r^{|L|} e^{iL\theta}$, where C is a z -independent constant. Thus, the OP distribution for nonzero L values becomes substantially inhomogeneous in the z direction only for $r/h \sim 1$, while in the regions $r/h \ll 1$ and $r/h \gg 1$ the OP is almost uniform over the film thickness (Fig. 7).

VI. CONCLUSION

In this paper we investigated theoretically the OP nucleation in a superconducting disk of finite radius R and thickness D , placed in an axially symmetric, nonuniform mag-

netic field. As an example, we considered the simplest case where such a nonuniform field is created by a point magnetic dipole magnetized perpendicular to the disk. This problem was studied both analytically and numerically to analyze the peculiarities of the phase-transition line $T_c(H)$ and the spatial structure of the OP in such hybrid systems. Now we summarize our important results.

Firstly, depending on the parameters of the magnetic particle and the external magnetic field H , there are two competing OP nucleation regimes, which determine the shape of the phase boundary $T_c(H)$. OP nucleation under the magnetic particle (the magnetic-dot-assisted regime) was shown to be energetically favorable for the intermediate H range ($H_1^* < H < H_2^*$). The switching fields H_1^* and H_2^* depend strongly on the film thickness D and on the parameter $N_f \sim m_0/(\Phi_0 h)$. An increase in the D value causes a shrinkage of the $|H_1^* - H_2^*|$ interval. For relatively small N_f values we find the critical thickness of the sample D_c corresponding to the complete disappearance of the magnetic-dot-assisted OP nucleation regime for any external field value. For magnetic dots with relatively small N_f values, or for $H < H_1^*$ or $H > H_2^*$ superconductivity always appears near the disk edge. We have shown that an increase in N_f above a certain critical value results in survival of the magnetic-dot-assisted superconductivity even for very thick films.

Secondly, switching between the OP nucleation regimes leads to a strong change in the oscillatory $T_c(H)$ behavior. The typical periods of the $T_c(H)$ oscillations can be estimated roughly as Φ_0/R^2 and Φ_0/h^2 for OP nucleation near the disk edge and the disk center, respectively. Thus, the shift of the OP maximum from the center of the disk to its edge is accompanied by an abrupt decrease in both the period and the amplitude of the Little-Parks oscillations for large-area samples ($R \gg h$). The Little-Parks oscillations in the magnetic-dot-assisted regime are shown to result from the switching between the giant vortex states with OP profiles modulated both in the lateral and transverse directions. An increase in the film thickness reduces the number of such vortex states, so that the vortex-free state is the most stable one over the widest range of the parameters H and D .

The superconductivity nucleates in the form of giant vortices only in systems with an axial symmetry. We expect that a variation of the sample shape can lead to a splitting of the single giant vortex into some single-quantum vortex configurations. Since the OP nucleation in thin superconducting film is shown to occur near the lines of zeros of $B_z(x, y)$, a tilt of the dot's magnetization will result in a deformation of the superconducting channels, which follow such lines and remain closed. As a result, the fluxoid quantization is also valid for S/F systems with nonaxial symmetry of the stray magnetic field. In all these cases the change of the total vorticity of the sample will remain discrete as before. Therefore, both types of the Little-Parks oscillations should be observed also in more complicated S/F hybrids, e.g., in superconducting disks and polygons with small and large magnetic dots with an arbitrary orientation of the magnetic moment. Thus, we believe that our simple model captures qualitatively the main underlying physics of the OP nucleation in various S/F hybrids.

ACKNOWLEDGMENTS

The authors would like to acknowledge David M. J. Taylor for his assistance in the preparation of the paper. This work was supported by the K. U. Leuven Research Fund GOA/2004/2 program, the Belgian IUAP, the Fund for Scientific Research—Flanders (F.W.O.-Vlaanderen), the bilat-

eral project BIL/05/25 between Flanders and Russia, by the Russian Foundation for Basic Research, by the program of Russian Academy of Sciences “Quantum Macrophysics,” by the BELSPO foundation (A.Yu.A.), by the Russian Science Support foundation, and by the Dynasty Foundation (A.S.M. and D.A.R.).

*Electronic address: alexei.aladyshkin@fys.kuleuven.be

- ¹W. A. Little and R. D. Parks, *Phys. Rev. Lett.* **9**, 9 (1962); R. D. Parks and W. A. Little, *Phys. Rev.* **133**, A97 (1964).
- ²H. J. Fink and A. G. Presson, *Phys. Rev.* **151**, 219 (1966); V. V. Moshchalkov, L. Gielen, C. Strunk, R. Jonckheere, X. Qiu, C. Van Haesendonck, and Y. Bruynseraede, *Nature (London)* **373**, 319 (1995); A. K. Geim, I. V. Grigorieva, S. V. Dubonos, J. G. S. Lok, J. C. Maan, A. E. Filippov, and F. M. Peeters, *ibid.* **390**, 259 (1997); V. A. Schweigert, and F. M. Peeters, *Phys. Rev. B* **57**, 13817 (1998); H. T. Jadallah, J. Rubinstein, and P. Sternberg, *Phys. Rev. Lett.* **82**, 2935 (1999); L. F. Chibotaru, A. Ceulemans, V. Bruyndoncx, and V. V. Moshchalkov, *Nature (London)* **408**, 833 (2000).
- ³Y. Otani, B. Pannetier, J. P. Nozières, and D. Givord, *J. Magn. Mater.* **126**, 622 (1993).
- ⁴M. Lange, M. J. Van Bael, Y. Bruynseraede, and V. V. Moshchalkov, *Phys. Rev. Lett.* **90**, 197006 (2003).
- ⁵D. S. Golubovic, W. V. Pogosov, M. Morelle, and V. V. Moshchalkov, *Phys. Rev. B* **68**, 172503 (2003); *Appl. Phys. Lett.* **83**, 1593 (2003).
- ⁶M. V. Milošević, and F. M. Peeters, *Phys. Rev. Lett.* **94**, 227001 (2005); M. V. Milošević, G. R. Berdiyrov, and F. M. Peeters, *ibid.* **95**, 147004 (2005).
- ⁷L. F. Chibotaru, A. Ceulemans, M. Morelle, G. Teniers, C. Carballeira, and V. V. Moshchalkov, *J. Math. Phys.* **46**, 095108 (2005).
- ⁸C. Carballeira, V. V. Moshchalkov, L. F. Chibotaru, and A. Ceulemans, *Phys. Rev. Lett.* **95**, 237003 (2005).
- ⁹Q. H. Chen, C. Carballeira, and V. V. Moshchalkov, *Phys. Rev. B* **74**, 214519 (2006).
- ¹⁰A. Yu. Aladyshkin, A. S. Mel’nikov, and D. A. Ryzhov, *J. Phys.: Condens. Matter* **15**, 6591 (2003).
- ¹¹S. B. Haley and H. J. Fink, *Phys. Rev. B* **53**, 3497 (1996).
- ¹²A. I. Buzdin and A. S. Mel’nikov, *Phys. Rev. B* **67**, 020503(R) (2003).
- ¹³A. Yu. Aladyshkin, A. I. Buzdin, A. A. Fraerman, A. S. Mel’nikov, D. A. Ryzhov, and A. V. Sokolov, *Phys. Rev. B* **68**, 184508 (2003).
- ¹⁴Z. Yang, M. Lange, A. Volodin, R. Szymczak, and V. V. Moshchalkov, *Nat. Mater.* **3**, 793 (2004).
- ¹⁵W. Gillijns, A. Yu. Aladyshkin, M. Lange, M. J. Van Bael, and V. V. Moshchalkov, *Phys. Rev. Lett.* **95**, 227003 (2005).
- ¹⁶J. Fritzsche, V. V. Moshchalkov, H. Eitel, D. Koelle, R. Kleiner, and R. Szymczak, *Phys. Rev. Lett.* **96**, 247003 (2006).
- ¹⁷A. Yu. Aladyshkin and V. V. Moshchalkov, *Phys. Rev. B* **74**, 064503 (2006).
- ¹⁸See, e.g., M. Lange, M. J. Van Bael, Y. Bruynseraede, and V. V. Moshchalkov, *Phys. Rev. Lett.* **90**, 197006 (2003).
- ¹⁹Yu. A. Izyumov, Yu. N. Proshin, and M. G. Khusainov, *Phys. Usp.* **45**, 109 (2002).
- ²⁰I. F. Lyuksyutov and V. L. Pokrovsky, *Adv. Phys.* **54**, 67 (2004).
- ²¹A. I. Buzdin, *Rev. Mod. Phys.* **77**, 935 (2005).
- ²²See, e.g., M. Tinkham, *Introduction to Superconductivity* (McGraw-Hill, New York, 1996), Chap. 4.
- ²³The symmetry of the solution of the linear differential equation (1) should be the same as the cylindrical symmetry of the magnetic field and sample boundaries. Non-axially-symmetrical solutions (e.g., single-quantum vortex configurations) appear only in nonlinear regime quite far from the phase-transition line.
- ²⁴L. Lapidus and G. F. Pinder, *Numerical Solution of Partial Differential Equations in Science and Engineering* (Wiley, New York, 1982), Chap. 5.